Growth-Associated Droplet Shrinkage for Bacterial Quantification, Growth Monitoring, and Separation by Ultrahigh-Throughput Microfluidics

Emilie Geersens, Stéphane Vuilleumier, Michaël Ryckelynck

ACS OMEGA

http://pubs.acs.org/journal/acsodf

Article

Growth-Associated Droplet Shrinkage for Bacterial Quantification, Growth Monitoring, and Separation by Ultrahigh-Throughput Microfluidics

Émilie Geersens, Stéphane Vuilleumier, and Michael Ryckelynck*

Cite This: *ACS Omega* 2022, 7, 12039−12047

Read Online

ACCESS | Metrics & More | Article Recommendations | Supporting Information

ABSTRACT: Microbiology still relies on en masse cultivation for selection, isolation, and characterization of microorganisms of interest. This constrains the diversity of microbial types and metabolisms that can be investigated in the laboratory also because of intercellular competition during cultivation. Cell individualization by droplet-based microfluidics prior to experimental analysis provides an attractive alternative to access a larger fraction of the microbial biosphere, miniaturizing the required equipment and minimizing reagent use for increased and more efficient analytical throughput. Here, we show that cultivation of a model two-strain bacterial community in droplets significantly reduces representation bias in the grown culture compared to batch cultivation. Further, and based on the droplet shrinkage observed upon cell proliferation, we provide proof-of-concept for a simple strategy that allows absolute quantification of microbial cells in a sample as well as selective recovery of microorganisms of interest for subsequent experimental characterization.

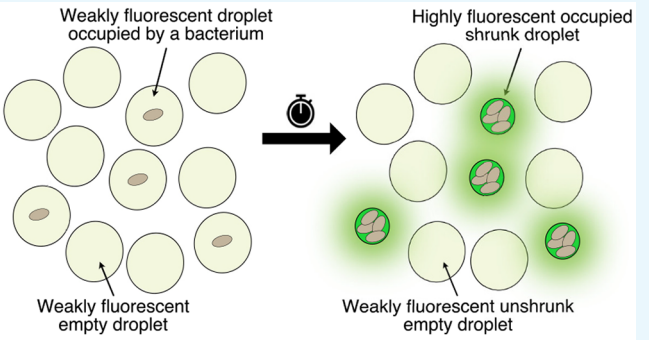

1. INTRODUCTION

Only a small proportion of the microbial biosphere has so far been experimentally explored and characterized in the laboratory by classical cultivation approaches.[1] Well-known major limitations responsible for this are natural competition between organisms differing in growth rates and metabolic capacities in batch cultures, and inhibitory effects due to molecules secreted during microbial growth. Recent progress in single-cell analytical technologies offers new ways of experimentally accessing the still largely unexplored majority of the microbial world.[2]

In current practice, laboratory cultures from environmental inocula containing a wide diversity of organisms with different growth rates and phenotypes will typically result in the enrichment and isolation of the few organisms best adapted to the imposed synthetic conditions, and thus overlook highly valuable biological information and material.[3]

Recent progress in single-cell analytical technologies offers new ways of addressing this issue and to better access the still largely unexplored majority of the microbial world,[2] by allowing to isolate each individual of a complex bacterial sample prior to cultivation and analysis. Today, working at single-cell resolution is greatly facilitated using microfluidics to handle very small volumes of liquid in a controlled manner.[4] In particular, droplet-based microfluidics allows extreme miniaturization of reaction vessels down to picoliter (or even femtoliter) volume.[5] With this technology, highly homogeneous water-in-oil droplets produced and manipulated at kHz frequencies can be used as inert individual cell compartments to allow growth without competition between cells.[6]

Following cell individualization, in-droplet growth can be monitored in several ways. For instance, cell proliferation can be monitored from label-free optical properties. For example, light scattering was used to study antibiotic resistance of bacteria in droplets,[7] although this approach may not be applicable to some types of organisms such as filamentous or slow-growing bacteria. The use of real-time image analysis was also reported, for instance for *Actinobacteria*.[8] However, this approach requires time-consuming image processing, has a relatively low signal-to-noise ratio, and depends on the position of the microorganism with respect to the focal plane. Similarly, Raman spectroscopy, also proposed for screening of bacterial cultures,[9] requires cell immobilization.[10] Fluorescence-based methods represent an efficient and sensitive alternative for growth monitoring, including approaches involving genetic modification with a gene coding for a fluorescent reporter such as the green fluorescent protein.[11] For complex communities

Received: January 12, 2022
Accepted: March 17, 2022
Published: March 30, 2022

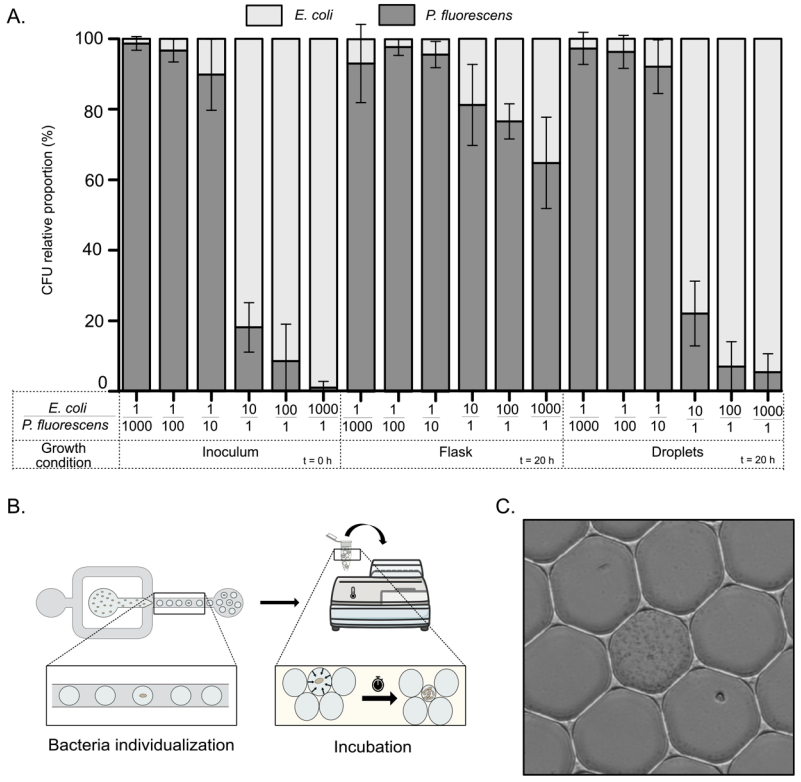

Figure 1. Bias in growth analysis of model bacterial cultures. (A) Mixtures of *E. coli* and *P. fluorescens* in ratios spanning 7 orders of magnitude were prepared and either inoculated into liquid M9 minimal medium in conventional flasks or dispersed into 20 pL of water-in-oil droplets (λ= 0.2) in the same medium prior to cultivation at 30 °C for 20 h. The composition of the starting inoculum and that of each culture at the final time point was analyzed by plating onto solid M9 minimal medium. Colonies were counted after 48 h incubation and assigned to *E. coli* (small nonfluorescent colonies) or *P. fluorescens* (large fluorescent colonies) (see Figure S2). Reported values represent the mean of three independent experiments, with error bars corresponding to ±1 standard deviation. (B) Microfluidic pipeline for cell individualization and incubation. (C) Micrograph of picoliter droplets following bacterial growth (scale: 5 μm).

(e.g., environmental samples), such genetic tools are not applicable, and in this case, fluorogenic dyes can be added to droplets to detect growth-associated reactions. For instance, resazurin is reduced to fluorescent resorufin by active metabolism.[12] Unfortunately, resorufin shows poor retention within droplets, and this prevents the fluorescence containment required for subsequent droplet analysis.[13]

In the present work, we explored the possibility of using monodisperse water-in-oil droplets to grow mixtures of bacteria with different growth rates without the biases inherent to batch cultivation. In the event, we showed that the previously observed growth-associated droplet shrinkage[14] could be exploited for straightforward, ultrahigh-throughput, and noninvasive quantification of bacteria and their growth. Key to this was inclusion of a carefully chosen nonexchangeable fluorescent dye in the medium to monitor droplet shrinkage. This approach was resolutive enough to distinguish strains with different growth rates and to separate and recover them by fluorescence-activated droplet sorting.

2. EXPERIMENTAL SECTION

2.1. Materials. All chemicals used in this study were purchased from Sigma-Aldrich unless specified otherwise. Microfluidic workstation, microfluidic chips (droplet generator and droplet sorter), and collection tubes were designed and prepared as described elsewhere.[15]

2YT medium consisted of (per L) 10 g of yeast extract, 16 g of tryptone, and 0−5 g of NaCl. M9 mineral medium consisted of (per L) 5.6 g of Na_2HPO_4, 3 g of KH_2PO_4, and 1 g of NH_4SO_4. After being autoclaved, the medium was supplemented with filter-sterilized solutions, affording final concentrations of 0.05% glucose, 20 μg/L vitamin B1, 1 mM $MgSO_4$, and 0.1 mg/mL L-leucine. Five grams/liter of casamino acids was also added for inoculum preparation in liquid culture in M9 medium. Solid media contained 15 g/L agar.

Escherichia coli (Ec) strain DH5α (NEB 5-alpha electrocompetent *E. coli* #C2989K) was transformed with plasmid pUC18 carrying the ampicillin-resistant gene according to the manufacturer's instructions. The *Pseudomonas fluorescens* strain (Pf) was a laboratory stock.

2.2. Bacterial Growth Measurements. Growth rate (μ, in h^{-1}) of strains Ec and Pf were determined from the slope of $\ln OD_{600}$ values in exponential phase through time. For differential growth measurements, starter cultures of each strain were prepared as overnight cultures in M9 medium. Strains Ec and Pf were diluted to the same OD_{600}, mixed in different ratios (1:10, 1:100, 1:1000), and used to inoculate 25 mL of liquid M9 medium in flasks or emulsified as described below. Inocula and grown populations (in flasks or in emulsions) were plated onto solid M9 mineral medium supplemented with 15 g/L Bacto agar and 5 g/L casamino acids and incubated for 48 h at 30 °C. Colonies were counted, and Ec and Pf strains were differentiated based on colony size (small Ec and large Pf colonies) on solid M9 medium, and fluorescence of Pf upon exposure to 312 nm UV light.

https://doi.org/10.1021/acsomega.2c00248
ACS Omega 2022, 7, 12039−12047

2.3. Bacteria Cultivation in Droplets. Samples (1 mL) from starter cultures obtained by overnight growth in M9 or 2YT liquid medium under agitation (150 rpm) were centrifuged for 5 min at 8000 rpm and resuspended in fresh medium, and their OD was measured at 600 nm (Jenway 7200 visible spectrophotometer). Cell suspensions were diluted in fresh medium to the expected droplet occupancy. For experiments in 20 pL droplets, bacterial suspensions were diluted in medium supplemented with 20 μg/mL Alexa Fluor 488 (Invitrogen) to an OD_{600} of 0.005, affording a λ value of 0.05. For other values of λ and droplet volume, dilutions were adapted accordingly.

Obtained diluted suspensions were transferred to 500 μL Eppendorf tubes containing a 5 × 2 mm stirrer bar (PTFE Stirrer Bar, Cowie) and sealed by a polydimethylsiloxane (PDMS) plug as described previously for collection tubes.[15] Bacteria were kept in suspension by stirring using a magnetic stirring plate placed next to the tube. The Eppendorf tube was connected to a Fluigent injection pump on one side and to the microfluidic chip on the other side. The diluted cell suspension was then dispersed in 2.5−20 pL of water-in-oil droplets by infusing a stream of Novec-7500 fluorinated oil (3M) supplemented with 3% fluorosurfactant[16] synthesized in-house into the device. Infusion rates of bacterial suspension and oil phase were adjusted to yield droplets of the desired volume. Emulsions were collected in tubes prior to transfer to a dry bath (Eppendorf ThermoStat C) set at 30 or 37 °C for the desired incubation time.

2.4. Droplet Analysis and Sorting. Following incubation, emulsions were reinjected into a custom droplet fluorescence analysis and sorting device as reported previously.[15] Droplets were spaced by a stream of surfactant-free Novec-7500 oil, and their green fluorescence was individually analyzed using an optical setup developed in the lab.[15] Both green fluorescence intensity and total droplet fluorescence content (integration of whole droplet fluorescence) were measured and used to compute the shrinkage index (see eq 2). For sorting, droplets of interest were deflected into the sorting channel by applying a 1200 V and 30 kHz AC electric field. Sorted droplets were recovered by addition of Novec-7500, and enrichment was controlled by plating recovered bacteria on solid M9 medium supplemented with casamino acids and analyzing colony morphology and fluorescence.

Droplet fluorescence was also analyzed using epi-fluorescence microscopy by deposition of droplets on a glass slide and imaging on a TiE (Nikon) platform equipped with a Lumencor LED light source. Bright-field and green fluorescence (excitation at 470 nm/emission at 490−530 nm) pictures were collected using an Orca-Flash4 (Hamamatsu Photonics K.K.) camera.

3. RESULTS AND DISCUSSION

3.1. Growth in Droplets Helps to Preserve the Original Bacterial Diversity in Samples. A key challenge for characterization of complex microbial populations (e.g., environmental samples) using cultivation approaches relates to competition for resources between organisms with unequal growth rates and exposure to bacterially produced growth inhibitory compounds. We investigated a simple two-strain model synthetic microbial community consisting of *Escherichia coli* and *Pseudomonas fluorescens*. The two strains are characterized by slightly different growth properties. *E. coli* grew best at 37 °C, whereas optimal growth of *P. fluorescens* was at 25−30 °C in both rich and minimal media, with growth rates differing by approximately 30% at 30 °C in M9 minimal medium (Figure S1). These rather modest differences were enough to strongly favor growth of *P. fluorescens* in flask cocultures of the two strains, significantly altering the final composition of the mixed culture. As shown in Figure 1A, flask incubations of both strains mixed in ratios spanning 7 orders of magnitude (i.e., from 1/10 to 1000/1, *E. coli*/*P. fluorescens*), in flasks containing M9 minimal medium for 20 h (corresponding to ∼14 and 20 generations for *E. coli* and *P. fluorescens*, respectively), strongly biased the composition of the final culture compared to the relative composition expected from the growth rates of the two strains determined in pure cultures of each strain (Figure S1).

We reasoned that individualizing bacteria prior to growth should reduce the bias observed in traditional flask cultures by limiting cell-to-cell competition. Droplet-based microfluidics allows objects such as cells to be encapsulated at very high frequency (production of hundreds to thousands of droplets per second) into highly homogeneous picoliter water-in-oil droplets.[17] Starting from an initial suspension, cells will distribute in droplets according to Poisson statistics.[18] It is thus possible to precisely predict the fraction of droplets occupied by one bacterium or more.[19] For instance, for an average concentration of 0.2 bacterium per droplet (i.e., 1 bacterium every 5 droplets), one can compute that 16% of the droplets will be occupied by one bacterium and 2% by more than 1 by solving eq 1:

$$P_{(x=k)} = \frac{e^{-\lambda}}{k!}\lambda^k \quad (1)$$

where λ is the average number of bacteria per compartment, k is the exact number of bacteria per compartment, and $P_{(x=k)}$ is the probability of having k bacteria per compartment. With this in mind, we emulsified, at a λ value of 0.05 (4.9% of occupied droplets), *E. coli*/*P. fluorescens* suspensions prepared in different ratios in minimal M9 medium prior to dispersing them into 20 pL of water-in-oil droplets. Emulsions were collected and incubated separately for 20 h at 30 °C (Figure 1B). Growth was observed with individualized bacteria developing monoclonal suspensions confined within the droplets (Figure 1C). Droplets were then retrieved, and the bacterial content of cultured emulsions was analyzed on agar plates. Most strikingly and unlike what was observed for flask-based cultivation, cultures grown in this way largely preserved the composition of the starting inoculum (Figure 1A). This confirmed that a simple approach exploiting droplet microfluidics represents an efficient way of amplifying the biomass in a sample while limiting biases (and associated information loss) due to competition between microorganisms in conventional batch cultures.

3.2. Detection of Bacterial Growth from Droplet Shrinkage. We noticed that bacterial growth in droplets was associated with significant droplet size reduction (Figure 1C and Figure S3). This had already been observed previously for both bacteria and yeast[14a,c] and was attributed to droplet-to-droplet water exchange as a consequence of cell growth and nutrient consumption by growing cells generating an osmotic gradient driving water transfer from occupied droplets to empty ones. We reasoned that this phenomenon may offer a new approach to determine cell counts in a sample in a

https://doi.org/10.1021/acsomega.2c00248
ACS Omega 2022, 7, 12039−12047

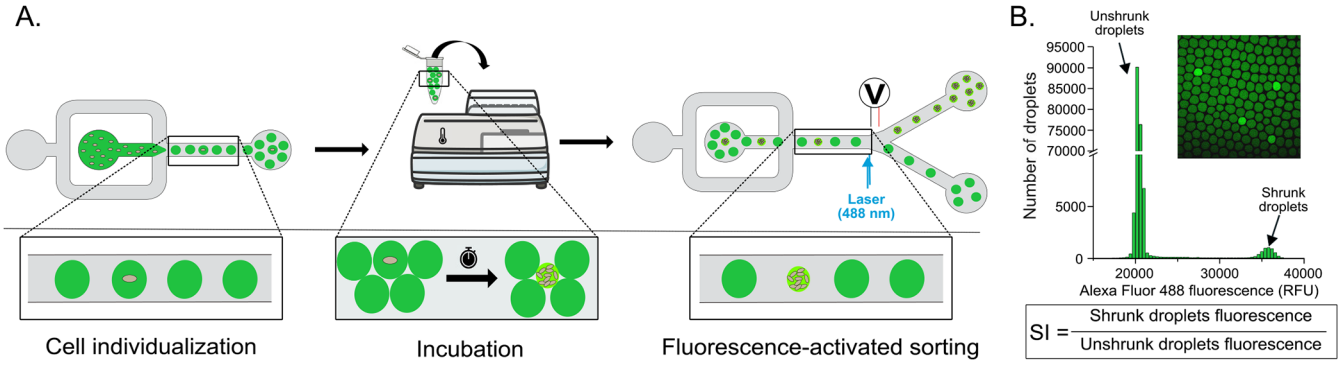

Figure 2. Shrinkage-based droplet analysis of bacterial growth. (A) Fluorescence-enabled, droplet-based microfluidic screening pipeline. Bacteria are individualized into 20 pL of water-in-oil droplets in the presence of the Alexa Fluor 488 fluorophore at 5 μg/mL final concentration (left), collected, and incubated from 2 to 20 h at the chosen temperature (middle). Droplets are then reinjected into a fluorescence-activated droplet sorting device (right) in which the fluorescence of each droplet is analyzed and used for sorting droplets displaying the fluorescence profile of interest. (B) Typical fluorescence profile obtained after incubation. Since not all droplets are occupied by bacteria, at least two distinct populations of droplets can be detected after incubation. Empty droplets conserve their original volume (unshrunk droplets) and show moderate fluorescence (~20 000 rfu). Droplets in which bacterial growth took place experience shrinkage (shrunk droplets), leading to an increase in fluorophore concentration and thus in fluorescence intensity (~35 000 rfu). Computing the fluorescence ratio of both populations yields the shrinkage index (here, shrinkage index ~ 1.75). The result can be confirmed by epifluorescence microscopy (inset).

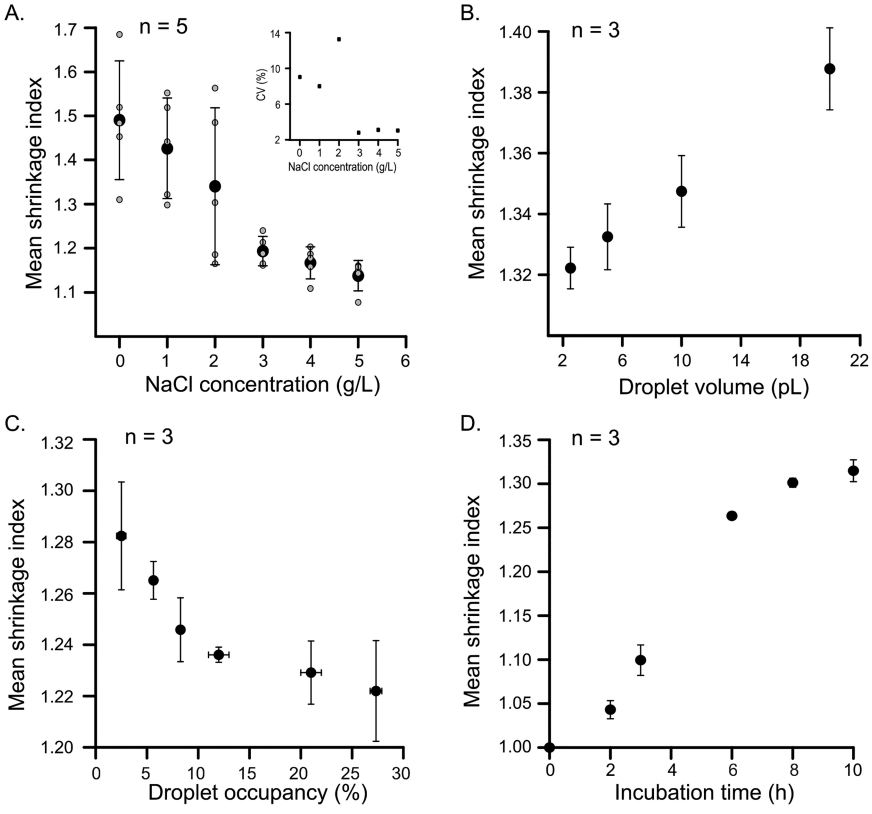

Figure 3. Main parameters affecting droplet shrinkage. The shrinkage index was determined as a function of four parameters: NaCl concentration (A), with evolution of the calculate coefficient of variation shown as an inset; droplet volume (B); droplet occupancy (C); and incubation time (D). Reported values represent the mean of 5 (gray circles in part A) or 3 (parts B–D) independent replicates, with errors bars corresponding to ±1 standard deviation.

ultrahigh-throughput manner, simply by adding a fluorescent dye to the medium (Figure 2).

Choice of the proper reporter dye was crucial. The dye should stay confined within droplets and become more concentrated as the volume of occupied droplets decreases. Previous work by us and others[13b,20] showed that retention of a dye in a droplet is directly correlated with its hydrophobicity: the more hydrophilic the dye, the better its retention. We chose the dye Alexa Fluor 488 because (i) its two sulfone groups are known to drastically favor droplet retention;[20] (ii) its high extinction coefficient and a quantum yield are close to 1; and (iii) its pH-insensitive fluorescence prevents any interference from growth-associated medium acidification.[21]

https://doi.org/10.1021/acsomega.2c00248
ACS Omega 2022, 7, 12039−12047

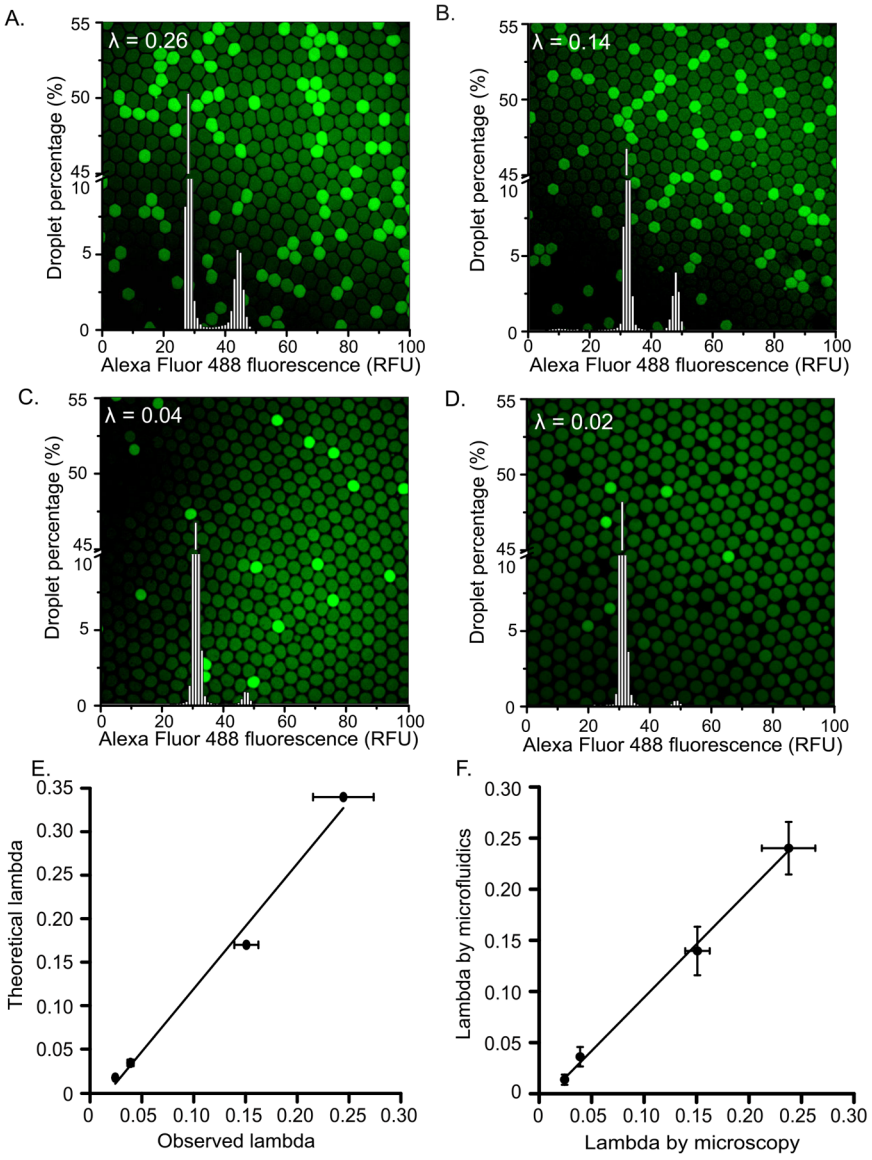

Figure 4. Droplet-based digital quantification of bacterial suspensions. Dilutions of *E. coli* were prepared in rich 2YT medium containing 3 g/L NaCl, supplemented with 5 μg/mL Alexa Fluor 488, and dispersed into 20 pL of water-in-oil droplets in the same medium. (A–D) After 15 h incubation at 37 °C, the fluorescence of each droplet was either analyzed with a high-throughput optical setup (bar charts) or evaluated by fluorescence microscopy (micrographs). Average numbers of bacteria per droplet (λ values) computed from experimental droplet occupancy using eq 3 are indicated. (E) Correlation between theoretical and observed λ values. (F) Correlation between digital high-throughput and microscopic analyses. Values reported in E and F represent the mean of three independent replicates, with error bars corresponding to ±1 standard deviation.

A suspension of *E. coli* was prepared at λ = 0.26 in 2YT-rich medium supplemented with Alexa 488 prior to being dispersed into droplets (Figure 2A). The resulting emulsion was collected, incubated for 20 h at 37 °C, and reinjected into an analysis and sorting device in which the Alexa Fluor 488 green fluorescence of each droplet was analyzed. As expected, droplet size reduction resulting from bacterial growth led to an increase in fluorescence intensity in the corresponding droplets (Figure 2B). Two distinct populations of droplets were observed, with shrunk droplets (average fluorescence of ~35 000 rfu) readily distinguishable from unshrunk droplets (~20 000 rfu). Of note, the two droplet populations displayed distinct maximum fluorescence but shared the same total fluorescence (Figure S4), confirming that both types of droplets contained the same total amount of dye, and that only its concentration changed upon droplet shrinkage. Our approach thus affords noninvasive, ultrahigh-throughput analysis (300 occupied droplets analyzed per second) of cells in a sample, and the use of a fluorescent reporter compatible with common filter sets also allows the fraction of droplets displaying bacterial growth using fluorescence microscopy to be defined (Figure 2B, inset).

3.3. Optimization of Droplet Shrinkage. The potential of droplet shrinkage for detection and quantification of bacterial growth was explored in more detail. In essence, water exchange between droplets is mainly driven by differences in solute concentrations.[14a,b] Specifically, peptone and tryptone in 2YT medium are consumed during bacterial growth, and their concentration should therefore decrease in droplets where bacterial growth takes place. Conversely, the concentration of NaCl in droplets should remain essentially the same. We reasoned, however, that salt may interfere with

https://doi.org/10.1021/acsomega.2c00248
ACS Omega 2022, 7, 12039−12047

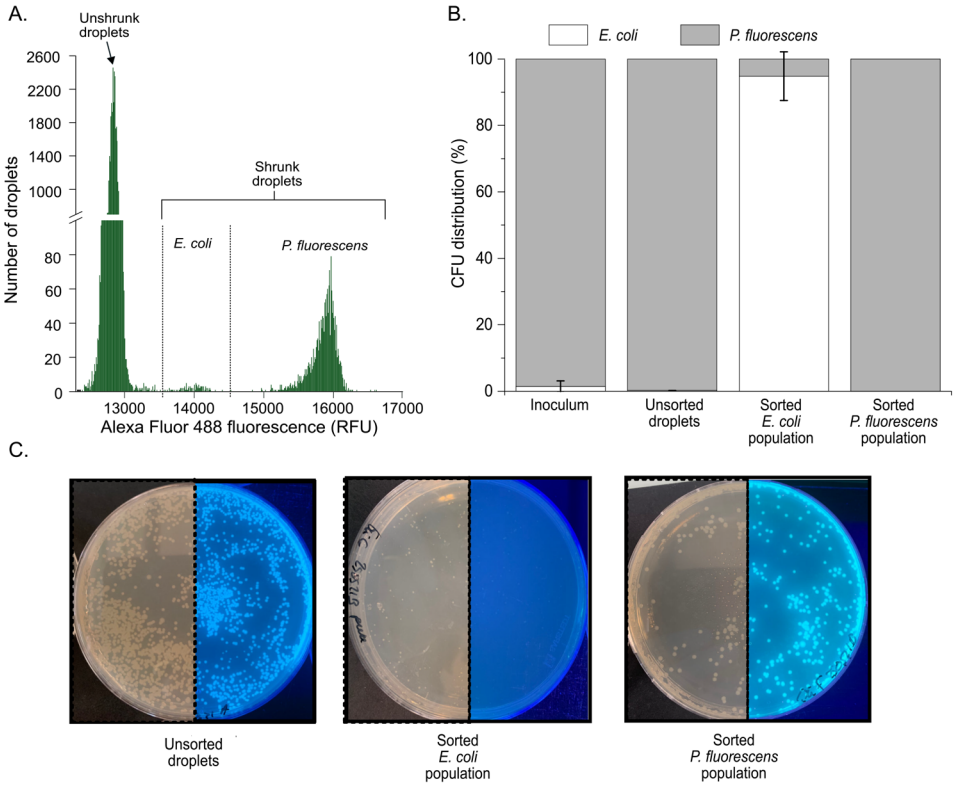

Figure 5. Microfluidic-enabled growth-associated subpopulation enrichment. (A) Fluorescence profile of a model mixed bacterial culture of slow-growing *E. coli* and fast-growing *P. fluorescens* in a 100:1 ratio, prepared in minimal M9 medium and supplemented with 5 μg/mL Alexa Fluor 488 prior to dispersing the mixture in 20 pL droplets and after 20 h incubation at 30 °C. Two additional populations of droplets were observed, with the most abundant displaying higher fluorescence (~16 000 rfu), clearly distinguishable from a minor, less fluorescent (~14 000 rfu) population. (B) Droplets sorted in A were plated on M9 minimal solid medium, and the nature of each colony was assigned to *E. coli* or *P. fluorescens* according to morphological and phenotypic features (see part C). Shown values represent the mean of two independent replicates, with error bars corresponding to ±1 standard deviation. (C) Slower-growing *E. coli* forms colonies smaller than those of *P. fluorescens* (left-hand side of Petri dishes photographed in normal light), and larger colonies of *P. fluorescens* appear fluorescent under UV light (right-hand side of Petri dishes; also see Figure S2).

droplet shrinkage by masking growth-dependent changes in the concentration of other solutes. To test this hypothesis, bacterial suspensions were prepared in 2YT medium supplemented with Alexa Fluor 488 and containing different concentrations of NaCl up to 5 g/L NaCl prior to being emulsified at $\lambda = 0.2$ in 2.5 pL droplets and incubated for 20 h at 37 °C. Droplets were then reinjected into an analysis device, and their individual fluorescence intensity was measured to compute the shrinkage index of each emulsion (Figure 2) using eq 2:

$$\text{shrinkage index} = \frac{\text{fluorescence}^{\text{shrunk droplets}}}{\text{fluorescence}^{\text{unshrunk droplets}}} \quad (2)$$

As anticipated, the lower the NaCl concentration, the larger the observed shrinkage (Figure 3A). In contrast, bacterial growth rate remained essentially unaffected at different concentrations of NaCl (Figure S5). However, the lowest NaCl concentrations (i.e., from 0 to 2 g/L), while most effective, were also associated with an important variability in the observed shrinkage (Figure 3A, inset), the origin of which remains to be better understood. From 3 g/L NaCl upward, shrinkage was much more reproducible, and this concentration was then used.

It was expected that, in addition to droplet occupancy, the extent of surface contact between occupied and bacteria-free droplets also plays a role in the magnitude of droplet shrinkage. To test this hypothesis, we evaluated shrinkage for droplet volumes ranging from 2.5 to 20 pL (i.e., droplet diameters ranging from ~17 to ~34 μm, respectively). We indeed found a direct correlation between droplet size and shrinkage index (Figure 3B). On this basis, it also seemed likely that the more an occupied droplet is surrounded by empty ones, the more exchange will be favored, and the more efficient the shrinkage will be. Indeed, varying droplet occupancy from 2.5 to 27.5% led to the expected decrease in shrinkage index (Figure 3C).

As a last optimization, we investigated the time required to observe a detectable effect in droplet size, as a crucial parameter for rapid identification of the presence of a live target bacterium (e.g., a pathogenic strain) in a sample. Accordingly, and using optimized parameters of salinity and droplet volume and occupancy (3 g/L NaCl, 20 pL droplets at $\lambda = 0.05$), a bacterial suspension in 2YT medium supplemented with Alexa Fluor 488 was emulsified, collected, and its shrinkage index determined at incubation times ranging from 2 to 10 h (Figure 3D). Under these conditions, droplets containing dividing bacteria were readily identified after an incubation time as short as 2 h. Shrinkage continued to increase with time, entering a plateau after 8 h.

3.4. Digital Titration, Analysis, and Sorting of Bacterial Suspensions. The microfluidic-assisted approach described here can be used to rapidly and precisely quantify cells in a sample in a universal and noninvasive manner by exploiting the same principles as digital droplet PCR.[22] As for

https://doi.org/10.1021/acsomega.2c00248
ACS Omega 2022, 7, 12039−12047

any digital method, sensitivity and precision are directly correlated with the number of compartments that can be analyzed, typically several millions of droplets in the present work.

Here, in order to evaluate the potential of our approach to precisely quantify cell counts in bacterial suspensions, we prepared dilutions of *E. coli* corresponding to theoretical λ values ranging from 0.017 to 0.34 (i.e., theoretical droplet occupancies ranging from 1.7 to 29%). Suspensions were emulsified in 20 pL droplets consisting of 2YT medium supplemented with Alexa Fluor 488 and containing 3 g/L NaCl and then incubated for 15 h at 37 °C. Droplet fluorescence was then analyzed either by reinjecting droplets into a fluorescence analysis device or by fluorescence microscopy (Figure 4). In both cases, droplet-containing bacteria were readily distinguishable from empty droplets (Figure 4A−D). Experimental λ values were computed from observed droplet occupancies using eq 3:

$$\lambda = -\ln(1 - \text{occupancy}) \quad (3)$$

These values were in excellent correlation (Pearson coefficient = 0.99) with those expected from the theory (Figure 4E). Moreover, online fluorescence measurements and microscopy yielded closely similar values (Pearson coefficient = 0.99, Figure 4F), suggesting that a simple common epifluorescence microscope is sufficient to quantify cell counts from a sample using our technology. However, online detection will be better suited for more accurate and automated measurements or for more complex downstream operations involving droplet sorting.

In this context, we sought to provide proof-of-principle of the potential of our approach for quantification and efficient sorting of different populations within a bacterial sample. To do this, a 1:100 *E. coli*/*P. fluorescens* mixed culture was diluted in minimum M9 medium supplemented with Alexa Fluor 488 and incubated at 30 °C for 20 h. Three populations of droplets were readily distinguished and sorted (Figure 5A). The least fluorescent population (∼12 500 rfu) was associated with empty unshrunk droplets, whereas the two others were predicted to represent droplet suspensions specific of each strain. Given that *E. coli* showed slower growth under the used conditions (Figure S5), we tentatively assigned it to the droplet suspension with an intermediate fluorescence increase (∼14 000 rfu). The most fluorescent population, i.e., that involving the largest droplet shrinkage (∼16 000 rfu), was predicted to correspond to droplets containing the best-growing bacteria, here, *P. fluorescens*. Fluorescent pyoverdine produced by *P. fluorescens* was not detectable on our optical setup (Figure S6), confirming that the detected fluorescence increases solely originated from Alexa Fluor 488 as a consequence of droplet shrinkage.

The identity of the different droplet populations was experimentally confirmed by sorting each droplet population using a fluorescence-activated droplet sorting device, prior to recovering bacteria and plating them on solid medium (Figure 5). As before, each colony was readily assigned to *E. coli* or *P. fluorescens* by comparison of colony morphology and fluorescence under UV light (Figures 5C and S5). *P. fluorescens* represented 98.8% of the total occupied droplets, a value close to the 1/100 ratio of *E. coli* to *P. fluorescens* used as inoculum. Moreover, bacteria recovered from sorted droplets were highly enriched in their respective strain, a feature especially interesting in the case of the slow-growing *E. coli* strain, which in batch mixed cultures together with *P. fluorescens* would have been lost for this reason (see Figure 1A, middle panel). Incidentally, these last data clearly indicate that our approach is not just useful in allowing bacterial growth to be detected. It is also quantitative to some extent: allowing to distinguish bacterial populations with different growth rates, it also affords the possibility not only to separate them based on their differences in growth rate but also to recover and enrich otherwise under-represented strains, including slow growers.

Worthy of note, the origin of the shrinkage observed here may differ from that previously reported with yeast, in which glucose consumption and conversion into oil-diffusive compounds were shown to be the main drivers.[14a] In the present case, the observed shrinkage may rather be due to assimilation of nutrients by growing cells. Such nutrient conversion into biomass likely creates a physicochemical mismatch between occupied droplets and surrounding empty ones, leading to water transfer from occupied to empty droplets. This hypothesis is consistent with our observation that shrinkage takes place in both rich and minimal media supplemented with the low concentrations of nutrients such as glucose as routinely used for bacterial cultivation. Consequently, and even if shrinkage amplitude is modest and therefore difficult to detect by droplet imaging techniques under our conditions, in contrast to when high glucose concentrations are used,[14a] the gain in sensitivity enabled by fluorescence-based detection allows even small shrinkage amplitudes (as quantified by the shrinkage index) to be detected and virtually any culture medium to be used, provided its salt content does not mask the physicochemical mismatch generated by bacterial growth.

4. CONCLUSIONS

We provided proof-of-principle for a novel bacterial cultivation and characterization approach, in which bacteria are first individualized in microfluidics-generated picoliter-size water-in-oil droplets. This allows biomass production while minimizing cultivation bias in samples containing different organisms. The oil surrounding aqueous droplet reactors isolates each cell with its own pool of nutrients, thereby ensuring access of slow growers to nutrients and limiting competition for resources. Cell compartmentalization also prevents diffusion of molecules secreted by bacteria that may inhibit growth.

Moreover, the observation that droplets occupied by cells decreased in size and volume upon bacterial growth was applied for the rapid detection (as short as 2 h) and monitoring of potentially any bacterial cell type in a ultrahigh-throughput and noninvasive way, by inclusion in the medium of an inert and nondiffusible fluorescent dye, as demonstrated in this work for both rich and minimal synthetic media. In effect, monitoring of droplet shrinkage, thus provides access to several digital microbiology approaches, such as quantification of cells in a sample by a simple yes/no (0/1) answer.

Of note, our approach only requires a microfluidic droplet generator to ensure proper emulsion monodispersity and limit droplet volume variations. Several benchtop devices and microfluidic chips are now commercially available for this purpose, and will facilitate implementation of the proposed approach. Further, droplet fluorescence analysis can already be performed with a simple and conventional epifluorescence microscope without the need for advanced analytical equip-

https://doi.org/10.1021/acsomega.2c00248
ACS Omega 2022, 7, 12039−12047

ment, further increasing the accessibility of the proposed approach.

■ ASSOCIATED CONTENT

Supporting Information

The Supporting Information is available free of charge at https://pubs.acs.org/doi/10.1021/acsomega.2c00248.

> Growth of *E. coli* and *P. fluorescens* under different conditions; phenotypic differentiation of *E. coli* and *P. fluorescens* colonies on solid M9 minimal medium; droplet shrinkage upon bacterial growth; fluorescence of *E. coli*-containing droplets after incubation; growth rate of *E. coli* for different NaCl concentrations in the medium; emission spectrum of *E. coli* and *P. fluorescens* for excitation at 488 nm (PDF)

■ AUTHOR INFORMATION

Corresponding Author

Michael Ryckelynck − *Université de Strasbourg, CNRS, Architecture et Réactivité de l'ARN, UPR 9002, 67000 Strasbourg, France;* orcid.org/0000-0002-2225-3733; Email: m.ryckelynck@unistra.fr

Authors

Émilie Geersens − *Université de Strasbourg, CNRS, Architecture et Réactivité de l'ARN, UPR 9002, 67000 Strasbourg, France; Université de Strasbourg, CNRS, Génétique Moléculaire, Génomique, Microbiologie, UMR 7156, 67000 Strasbourg, France;* orcid.org/0000-0002-0655-7657

Stéphane Vuilleumier − *Université de Strasbourg, CNRS, Génétique Moléculaire, Génomique, Microbiologie, UMR 7156, 67000 Strasbourg, France;* orcid.org/0000-0003-2232-7023

Complete contact information is available at: https://pubs.acs.org/10.1021/acsomega.2c00248

Notes

The authors declare the following competing financial interest(s): E.G. and M.R. have filed a patent application to protect the technology disclosed in this publication.

■ ACKNOWLEDGMENTS

This work received financial support from Agence Nationale de la Recherche (dehalofluidX project ANR-17-CE07-0009, which also funded E.G.'s PhD thesis). Performed within Interdisciplinary Thematic Institute "IMCBio" (ITI 2021-2028 program of University of Strasbourg, CNRS and Inserm), this work was also supported by IdEx Unistra (ANR-10-IDEX-0002), SFRI-STRAT'US project (ANR-20-SFRI0012), EUR IMCBio (ANR-17-EURE-0023) under the framework of the French Investments for the Future Program, the previous LabEx NetRNA (ANR-10-LABX-0036), and was also supported by Centre National de la Recherche Scientifique (CNRS), Université de Strasbourg, and its Initiative of Excellence (IdEx).

■ REFERENCES

(1) Overmann, J.; Abt, B.; Sikorski, J. Present and future of culturing bacteria. *Annu. Rev. Microbiol.* **2017**, *71*, 711−730.

(2) Rosenthal, K.; Oehling, V.; Dusny, C.; Schmid, A. Beyond the bulk: disclosing the life of single microbial cells. *FEMS Microbiol. Rev.* **2017**, *41*, 751−780.

(3) (a) Ghoul, M.; Mitri, S. The ecology and evolution of microbial competition. *Trends Microbiol.* **2016**, *24*, 833−845. (b) Nagy, K.; Abraham, A.; Keymer, J. E.; Galajda, P. Application of microfluidics in experimental ecology: the importance of being spatial. *Front. Microbiol.* **2018**, *9*, 496.

(4) (a) Autour, A.; Ryckelynck, M. Ultrahigh-throughput improvement and discovery of enzymes using droplet-based microfluidic screening. *Micromachines* **2017**, *8*, 128. (b) Kaminski, T. S.; Scheler, O.; Garstecki, P. Droplet microfluidics for microbiology: techniques, applications and challenges. *Lab Chip* **2016**, *16*, 2168−2187.

(5) Scheler, O.; Postek, W.; Garstecki, P. Recent developments of microfluidics as a tool for biotechnology and microbiology. *Curr. Opin. Biotechnol.* **2019**, *55*, 60−67.

(6) Huys, G. R.; Raes, J. Go with the flow or solitary confinement: a look inside the single-cell toolbox for isolation of rare and uncultured microbes. *Curr. Opin. Microbiol.* **2018**, *44*, 1−8.

(7) (a) Liu, X.; Painter, R. E.; Enesa, K.; Holmes, D.; Whyte, G.; Garlisi, C. G.; Monsma, F. J.; Rehak, M.; Craig, F. F.; Smith, C. A. High-throughput screening of antibiotic-resistant bacteria in picodroplets. *Lab Chip* **2016**, *16*, 1636−1643. (b) Pacocha, N.; Boguslawski, J.; Horka, M.; Makuch, K.; Lizewski, K.; Wojtkowski, M.; Garstecki, P. High-throughput monitoring of bacterial cell density in nanoliter droplets: label-free detection of unmodified Gram-positive and Gram-negative bacteria. *Anal. Chem.* **2021**, *93*, 843−850.

(8) Zang, E.; Brandes, S.; Tovar, M.; Martin, K.; Mech, F.; Horbert, P.; Henkel, T.; Figge, M. T.; Roth, M. Real-time image processing for label-free enrichment of *Actinobacteria* cultivated in picolitre droplets. *Lab Chip* **2013**, *13*, 3707−3713.

(9) Wang, X.; Ren, L.; Su, Y.; Ji, Y.; Liu, Y.; Li, C.; Li, X.; Zhang, Y.; Wang, W.; Hu, Q.; et al. Raman-Activated droplet sorting (RADS) for label-free high-throughput screening of microalgal single-cells. *Anal. Chem.* **2017**, *89*, 12569−12577.

(10) McIlvenna, D.; Huang, W. E.; Davison, P.; Glidle, A.; Cooper, J.; Yin, H. Continuous cell sorting in a flow based on single cell resonance Raman spectra. *Lab Chip* **2016**, *16*, 1420−1429.

(11) Martin, K.; Henkel, T.; Baier, V.; Grodrian, A.; Schon, T.; Roth, M.; Kohler, J. M.; Metze, J. Generation of larger numbers of separated microbial populations by cultivation in segmented-flow microdevices. *Lab Chip* **2003**, *3*, 202−207.

(12) Kaushik, A. M.; Hsieh, K.; Chen, L.; Shin, D. J.; Liao, J. C.; Wang, T. H. Accelerating bacterial growth detection and antimicrobial susceptibility assessment in integrated picoliter droplet platform. *Biosens. Bioelectron.* **2017**, *97*, 260−266.

(13) (a) Courtois, F.; Olguin, L. F.; Whyte, G.; Theberge, A. B.; Huck, W. T.; Hollfelder, F.; Abell, C. Controlling the retention of small molecules in emulsion microdroplets for use in cell-based assays. *Anal. Chem.* **2009**, *81*, 3008−3016. (b) Gruner, P.; Riechers, B.; Semin, B.; Lim, J.; Johnston, A.; Short, K.; Baret, J.-C. Controlling molecular transport in minimal emulsions. *Nat. Commun.* **2016**, *7*, 10392.

(14) (a) Boitard, L.; Cottinet, D.; Kleinschmitt, C.; Bremond, N.; Baudry, J.; Yvert, G.; Bibette, J. Monitoring single-cell bioenergetics via the coarsening of emulsion droplets. *Proc. Natl. Acad. Sci. U S A* **2012**, *109*, 7181−7186. (b) Hofmann, T. W.; Hanselmann, S.; Janiesch, J. W.; Rademacher, A.; Bohm, C. H. Applying microdroplets as sensors for label-free detection of chemical reactions. *Lab Chip* **2012**, *12*, 916−922. (c) Woronoff, G.; Nghe, P.; Baudry, J.; Boitard, L.; Braun, E.; Griffiths, A. D.; Bibette, J. Metabolic cost of rapid adaptation of single yeast cells. *Proc. Natl. Acad. Sci. U S A* **2020**, *117*, 10660−10666.

(15) Bouhedda, F.; Cubi, R.; Baudrey, S.; Ryckelynck, M. μIVC-Seq: A Method for ultrahigh-throughput development and functional characterization of small RNAs. *Methods Mol. Biol.* **2021**, *2300*, 203−237.

(16) Holtze, C.; Rowat, A. C.; Agresti, J. J.; Hutchison, J. B.; Angile, F. E.; Schmitz, C. H. J.; Koster, S.; Duan, H.; Humphry, K. J.; Scanga,

R. A.; et al. Biocompatible surfactants for water-in-fluorocarbon emulsions. *Lab Chip* **2008**, *8*, 1632−1639.
(17) Najah, M.; Griffiths, A. D.; Ryckelynck, M. Teaching single-cell digital analysis using droplet-based microfluidics. *Anal. Chem.* **2012**, *84*, 1202−1209.
(18) (a) Clausell-Tormos, J.; Lieber, D.; Baret, J.-C.; El-Harrak, A.; Miller, O. J.; Frenz, L.; Blouwolff, J.; Humphry, K. J.; Koster, S.; Duan, H.; et al. Droplet-based microfluidic platforms for the encapsulation and screening of mammalian cells and multicellular organisms. *Chem. Biol.* **2008**, *15*, 427−437. (b) Mazutis, L.; Araghi, A. F.; Miller, O. J.; Baret, J.-C.; Frenz, L.; Janoshazi, A.; Taly, V.; Miller, B. J.; Hutchison, J. B.; Link, D.; et al. Droplet-based microfluidic systems for high-throughput single DNA molecule isothermal amplification and analysis. *Anal. Chem.* **2009**, *81*, 4813−4821.
(19) Collins, D. J.; Neild, A.; deMello, A.; Liu, A. Q.; Ai, Y. The Poisson distribution and beyond: methods for microfluidic droplet production and single cell encapsulation. *Lab Chip* **2015**, *15*, 3439−3459.
(20) Woronoff, G.; El Harrak, A.; Mayot, E.; Schicke, O.; Miller, O. J.; Soumillion, P.; Griffiths, A. D.; Ryckelynck, M. New generation of amino coumarin methyl sulfonate-based fluorogenic substrates for amidase assays in droplet-based microfluidic applications. *Anal. Chem.* **2011**, *83*, 2852−2857.
(21) https://www.thermofisher.com/fr/fr/home/references/molecular-probes-the-handbook/technical-notes-and-product-highlights/the-alexa-fluor-dye-series.html (accessed on March 21, 2021).
(22) Quan, P. L.; Sauzade, M.; Brouzes, E. dPCR: A technology review. *Sensors* **2018**, *18*, 1271.

https://doi.org/10.1021/acsomega.2c00248
ACS Omega 2022, 7, 12039−12047